Planetary and Space Science 59 (2011) 1659–1664

Contents lists available at ScienceDirect

Planetary and Space Science

journal homepage: www.elsevier.com/locate/pss

Rapid Communication

On the role of dust in the lunar ionosphere

T.J. Stubbs [a,b,f,*,1], D.A. Glenar [c,b,f], W.M. Farrell [b,f], R.R. Vondrak [b,f], M.R. Collier [b,f], J.S. Halekas [b,f], G.T. Delory [d,e,f]

[a] Center for Research and Exploration in Space Science and Technology, University of Maryland, Baltimore County, MD, USA
[b] NASA Goddard Space Flight Center, Greenbelt, MD, USA
[c] New Mexico State University, Las Cruces, NM, USA
[d] Space Sciences Laboratory, University of California, Berkeley, CA, USA
[e] NASA Ames Research Center, Moffett Field, CA, USA
[f] NASA Lunar Science Institute, NASA Ames Research Center, Moffett Field, CA, USA

ARTICLE INFO

Article history:
Received 21 March 2011
Received in revised form
28 May 2011
Accepted 30 May 2011
Available online 13 June 2011

Keywords:
Moon
Lunar ionosphere
Radio occultation
Dust-electrons
Luna 19
Apollo 15
Horizon glow

ABSTRACT

Radio occultation measurements from the Soviet Luna 19 mission suggest that electron concentrations above the sunlit lunar surface can be significantly higher than that expected from either the photo-ionization of exospheric neutrals or any other well-known process. These measurements were used to infer the electron column concentrations above the lunar limb as a function of tangent height, which surprisingly indicated peak concentrations of $\sim 10^3\ \mathrm{cm}^{-3}$ at ~ 5 km altitude. It has been speculated that electrically charged exospheric dust could contribute to such electron populations. This possibility is examined here using the exospheric dust abundances inferred from Apollo 15 coronal photographs to estimate the concentration of electrons produced by photo- and secondary emission from dust. These estimates far exceed the electron concentrations predicted by any other suggested mechanism, and are within a factor of ≈ 20 of those inferred from the Luna 19 measurements. It is possible that this discrepancy is due to an under-estimate in dust grain capacitances and/or the presence of much higher exospheric dust abundances during the Luna 19 measurements. These results suggest that electrons emitted from exospheric dust could be responsible for the Luna 19 measurements, and that this process could dominate the formation and evolution of the lunar ionosphere.

© 2011 Elsevier Ltd. All rights reserved.

1. Introduction

The Soviet Luna 19 and 22 spacecraft conducted a series of radio occultation measurements to determine the line-of-sight electron column concentration N_e, or total electron content (TEC), above the limb of the Moon as a function of tangent height (e.g., Vasil'ev et al., 1974; Vyshlov, 1976). From these measurements they inferred the presence of a "lunar ionosphere" above the sunlit lunar surface with peak electron concentrations $n_e \sim 500$–$1000\ \mathrm{cm}^{-3}$ and scale heights of ~ 10–30 km. These values are broadly consistent with those inferred from lunar occultation measurements of the Crab Nebula in which radio waves were refracted in the vicinity of the Moon (e.g., Elsmore, 1957; Vyshlov and Savich, 1979). These observations are particularly intriguing, and somewhat controversial, since there is no well-established physical mechanism for producing such high electron concentrations in the lunar environment (see review by Imamura et al., 2010). Despite the existence of exospheric neutrals on the lunar dayside ($\sim 10^5\ \mathrm{cm}^{-3}$), the long photo-ionization time-scales (~ 10–100 days) combined with rapid ion pick-up by the solar wind (~ 1 s) should limit the associated electron concentrations to only $\sim 1\ \mathrm{cm}^{-3}$ (Stern, 1999). Other suggested mechanisms include plasma trapping by lunar crustal magnetic fields (Savich, 1976) and the photoemission of electrons from the surface (Bauer, 1996). More recently, Imamura et al. (2008) speculated that charged exospheric dust might be accompanied by a substantial population of electrons.

Lunar exospheric dust exposed to solar ultraviolet (UV), as considered here, tends to acquire a positive electric charge due to the dominance of photoemission currents. The photo- and secondary electrons emitted from dust are expected to have an effective temperature of only ~ 1–5 eV, so the vast majority of electrons will not be energetic enough to escape the dust grains' attractive electric potential of ~ 5 V (Goertz, 1989). Since these electrons are both emitted and mostly confined to a region close to the dust grains, we refer to them as "dust-electrons". Any escaping electrons will either be picked-up by the solar wind, or captured by neighboring dust grains. In contrast, lunar exospheric dust in shadow will tend to acquire a negative charge due to the dominance of plasma electron

* Corresponding author at: NASA Goddard Space Flight Center, Mail Code 695, Greenbelt, MD 20771, USA. Tel.: +1 301 286 1524.
E-mail address: Timothy.J.Stubbs@NASA.gov (T.J. Stubbs).
[1] Formerly at Goddard Earth Sciences and Technology Center, University of Maryland, Baltimore County, MD, USA.

0032-0633/$ - see front matter © 2011 Elsevier Ltd. All rights reserved.
doi:10.1016/j.pss.2011.05.011

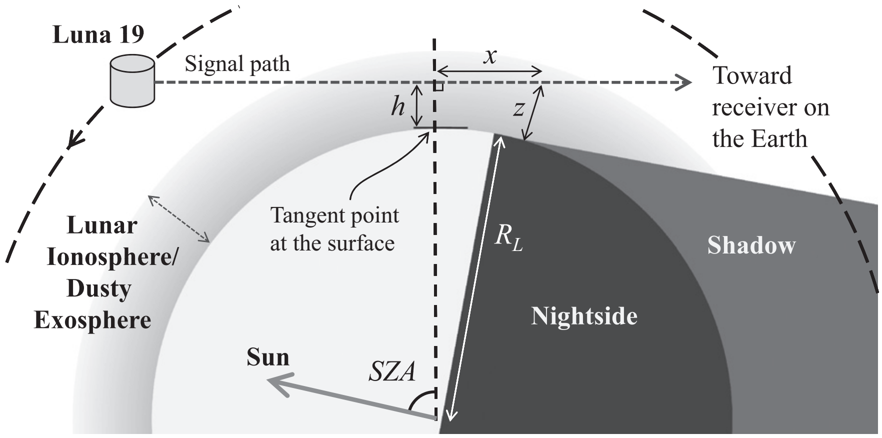

Fig. 1. A sketch of the Luna 19 radio occultation viewing geometry (Not To Scale).

currents, such that all secondary electrons emitted from the dust grains will be repelled, and so rapidly escape to be picked-up by the solar wind.

Here we make the first predictions for the electron concentrations produced by photo- and secondary emission from exospheric dust extending to high-altitudes ($\sim$10–100 km). This is done using the line-of-sight dust column concentrations inferred from the lunar horizon glow detected in Apollo 15 coronal photographs (McCoy, 1976). Therefore, these initial dust-electron predictions are independent of any particular exospheric dust transport or ejection mechanism. A comparison with predictions from some of the previously proposed mechanisms indicates that dust-electrons could be the dominant contributor to the Luna electron measurements. This suggests a new paradigm in which exospheric dust can dominate the formation and evolution of the lunar ionosphere.

2. The Luna radio occultation measurements

The Luna dual-frequency radio occultation, or dispersion interferometry, experiments involved the simultaneous transmission of two coherent monochromatic signals from the spacecraft in lunar orbit toward a receiver on the Earth, as illustrated in Fig. 1. The wavelengths used were 0.32 m (940 MHz: UHF) and 0.08 m (3.75 GHz: S-band). The reduced phase difference derived from these measurements is proportional to the electron column concentration along the line-of-sight between the transmitter and the receiver (Vasil'ev et al., 1974). As the Luna spacecraft orbited the Moon, a series of measurements at different tangent heights (altitudes above the limb) were acquired with each limb traversal to/from the lunar far side, as observed from the Earth. At tangent heights $>\sim$50–100 km, there appeared to be no perturbation from electrons of lunar origin, and so this was regarded as a measurement of the background due to the Earth's ionosphere, interplanetary space (solar wind), and other sources. By comparing the reduced phase difference at lower tangent heights with this background, it was possible to derive electron column concentrations through the lunar ionosphere (see Vasil'ev et al., 1974, for more details). Luna 19 orbited at an altitude of $\sim$140 km, so it was continuously above the detectable part of the lunar ionosphere, as indicated in Fig. 1.

In order to be detectable using this technique the lunar ionosphere must have concentrations greater than the interplanetary background. Accounting for changes in the Earth's ionosphere is also a significant issue, but Vasil'ev et al. (1974) argue that during undisturbed intervals the variations occur at an almost constant rate, and so can be easily subtracted.

At the UHF and S-band frequencies used in this experiment, it is essentially only the plasma electrons that are mobile enough to respond to the radio waves' electric field, and thus contribute to the reduced phase difference. Also, these radio frequencies are much higher than any resonant plasma frequencies in the lunar ionosphere ($<$2.5 MHz), and so the radio waves would not be reflected.

We focus on the electron column concentrations inferred from the Luna 19 radio occultation measurements acquired on 11 June 1972 by Vasil'ev et al. (1974), which are reproduced in Fig. 2a and hereafter referred to as the Luna 19 measurements. These observations occurred above a limb tangent point on the Moon with selenographic coordinates of $\sim$40°S, 96.3°E, corresponding to a solar zenith angle $SZA \approx 89^\circ$ near the sunrise terminator. These measurements were selected because: (i) they had the best available estimate of uncertainties; (ii) the tangent point was close to the sunrise terminator, and so could be readily compared with the Apollo 15 exospheric dust observations; and (iii) they were reasonably representative of all the Luna 19 and 22 observations. The Earth's ionosphere was likely quiet during this interval, as indicated by a low $\langle K_P$ index$\rangle$ (see Table 1), while the detection threshold appeared to be relatively high at $\sim 10^{10}$ cm^{-2}. The Luna 19 and Apollo 15 measurements both occurred when the Moon was in the solar wind (see Fig. 2b); this is relevant since the charging (and possibly the transport) of exospheric dust is dependent on plasma conditions (Goertz, 1989; Stubbs et al., 2006).

3. Comparison between Luna 19 and Apollo 15 line-of-sight measurements

For this comparison we use exospheric dust column concentrations N_d inferred from the lunar horizon glow detected in Apollo 15 coronal photographs taken above the sunrise terminator (see Fig. 1 from McCoy, 1976). The dust column concentrations, hereafter referred to as the Apollo 15 measurements, are calculated assuming scattering by monodisperse dust grains with radii a=0.1 μm, as shown in Fig. 3a by black circles and lines (see McCoy, 1976, for more details). Tangent heights were estimated using the solar elongation angles in Table 5 of McCoy (1976), the known pointing geometry, and the mean orbital altitude of 110 km for the Apollo 15 command module. No quantitative estimates of the uncertainties were provided in the McCoy (1976) analysis, but the Apollo 15 measurements should clearly be regarded as order-of-magnitude estimates.

In order to understand the processes involved with these phenomena, and readily convert between column and volumetric

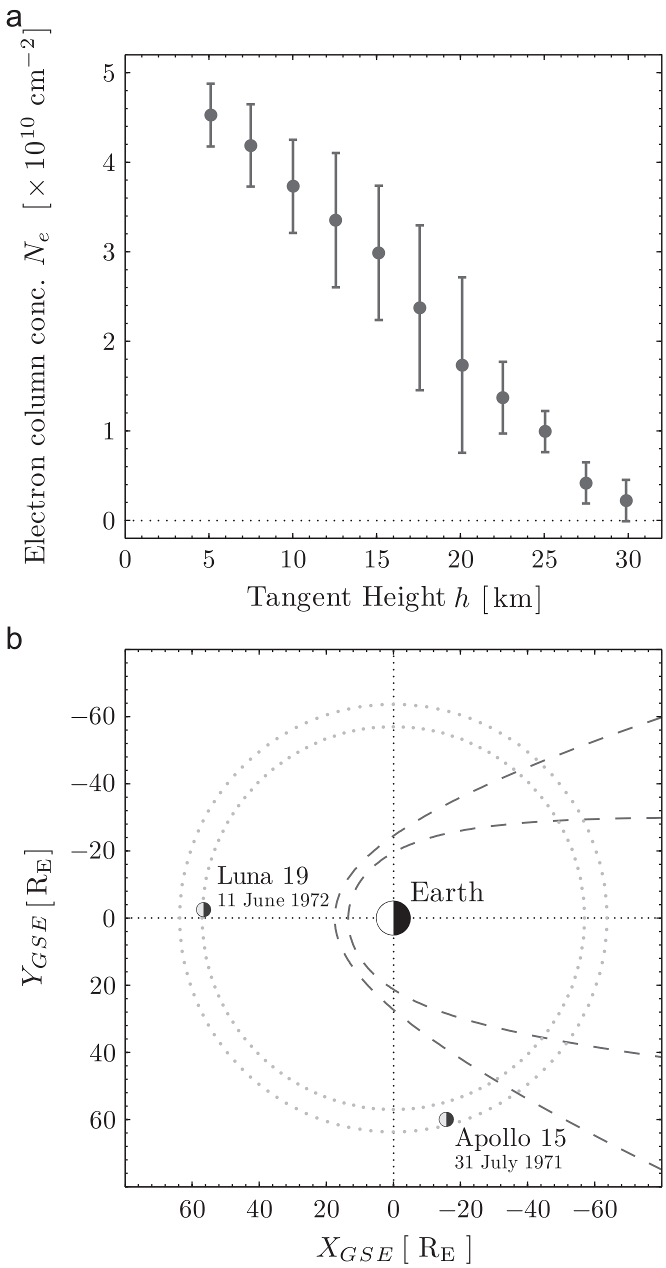

Fig. 2. (a) Electron column concentrations N_e inferred from Luna 19 radio occultation measurements with estimated uncertainties (Vasil'ev et al., 1974) and (b) location of the Moon in the ecliptic plane during the Luna 19 and Apollo 15 observations. Dotted circles show the lunar orbit range, and dashed lines represent the magnetopause (inner boundary) and bow shock (outer boundary) under typical conditions – this indicates that the Moon was in the solar wind for both these observations.

Table 1
Average conditions for the Earth's magnetosphere/ionosphere (K_P index) and solar UV ($F_{10.7}$ index).

Mission	Observation interval	$\langle K_P \rangle$	$\langle F_{10.7} \rangle$
Luna 19	11 June 1972 $\approx$ 05:00–09:00 UT	≤ 1	143.2
Apollo 15	31 July 1971 $\approx$ 18:43 UT	4−	113.2
Kaguya	14 Sept 2007–10 June 2009	$\approx 1+$	≈ 70
Space age	1964–2009	$\approx 2+$	≈ 125

concentrations, it is extremely useful to fit functional forms to these measurements. To a good approximation, we find that the exospheric dust concentrations inferred from the Apollo 15 measurements decrease exponentially with altitude z, such that

$$n_d(z) = n_{d0} \exp\left(-\frac{z}{H_d}\right); \tag{1}$$

where n_{d0} is the concentration at the surface, and H_d is the scale height for exospheric dust.

From Eq. (1) we can derive an analytical solution for the dust column concentration along a tangential line-of-sight. By following a similar approach to Collier and Stubbs (2009), it can be shown that

$$z = \sqrt{x^2 + (R_L + h)^2} - R_L \approx h + \frac{x^2}{2(R_L + h)}, \tag{2}$$

where h is tangent height and x is the distance along the tangential line-of-sight, as illustrated in Fig. 1. We are able to use the approximation in Eq. (2) since the path length through the layer of exospheric dust is much smaller than the lunar radius $R_L = 1738$ km. For scale heights of $\sim$10–20 km, the effective path length will be only be a few hundred km at most, so the requirement that $x \ll R_L$ is always satisfied. If we assume that the exospheric dust distribution is spherically symmetric about the center of the Moon, at least along the tangential line-of-sight, then we can substitute Eq. (1) into (2) to derive the dust column concentration,

$$\begin{aligned} N_d(h) &= n_{d0} \exp\left(-\frac{h}{H_d}\right) \int_{-\infty}^{\infty} \exp\left[-\frac{x^2}{2H_d(R_L + h)}\right] dx \\ &= n_{d0} \sqrt{2\pi H_d (R_L + h)} \exp\left(-\frac{h}{H_d}\right). \end{aligned} \tag{3}$$

In Eq. (3) we can integrate to infinity since the contribution to $N_d(h)$ from dust at $|x|$ greater than a few hundred km is negligible (see Chamberlain, 1978). Using Eq. (3), we find a good fit to the McCoy (1976) estimates using $n_{d0} = 0.1$ cm^{-3} and $H_d = 15$ km (dashed line in Fig. 3a), which we refer to as the Apollo 15 fit N_{d_A15}.

Now we address the critical step of converting between dust and dust-electron concentrations. Dust grains in the lunar exosphere can be exposed to solar UV and various space plasma populations, which cause them to become electrically charged (Goertz, 1989). For the size and concentration of dust grains considered here ($a \approx 0.1$ μm and $n_d < \sim 0.1$ cm^{-3}), we can assume that they are much smaller than both the inter-grain distance d and the local Debye length λ_D (i.e., $a \ll d \ll \lambda_D$). This, combined with an assumption that the dust grains are spherical, means that the charge on each dust grain is given by

$$q_d = C_d \phi_d = 4\pi\varepsilon_0 a \phi_d, \tag{4}$$

where ϕ_d is the potential difference between the grain and surrounding plasma (not necessarily in equilibrium) and C_d is the capacitance of the dust grain (Goertz, 1989). It should be appreciated that a spherical grain shape gives the minimum capacitance per unit volume (or unit mass), and that even the very smallest grains in the lunar regolith can be highly irregular in shape (e.g., Park et al., 2006). This means that $C_d = 4\pi\varepsilon_0 a$ should be regarded as a lower limit for dust grain capacitance, since grains with more realistic shapes could hold much more charge for a given ϕ_d.

Since the dusty plasma must be quasi-neutral, there will be sufficient ambient electrons/ions to balance the charge accumulated by the dust grains. Any dust present during the Luna 19 and Apollo 15 measurements would have been exposed to both solar UV and solar wind plasma, which, in equilibrium, would have charged it to $\phi_d \sim 5$ V positive and caused it to be surrounded by a cloud of at least $\sim$350 mostly photo-emitted electrons (Whipple, 1981).

We note that collective charging effects in this case can be neglected because: (i) the dominant charging current is due to

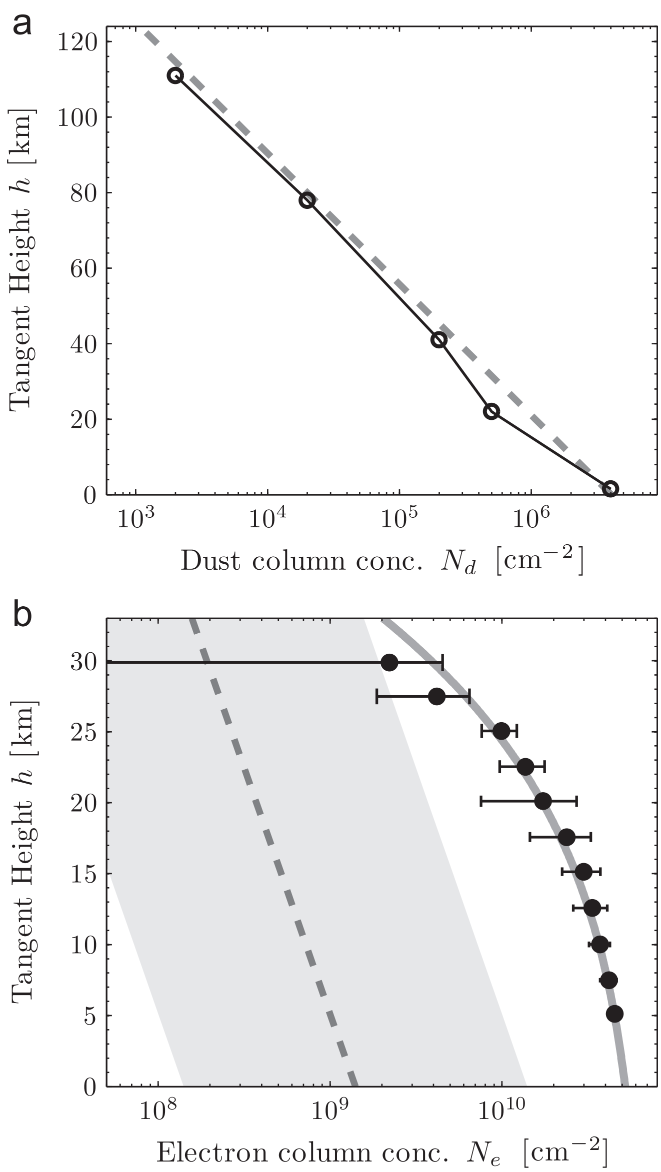

Fig. 3. (a) Exospheric dust column concentrations N_d inferred from Apollo 15 coronal photography (black circles and lines) by McCoy (1976). Dashed line shows a fit using Eq. (3). (b) Dust-electron predictions N_{de} (dashed lines) with estimated uncertainties (gray shading) compared with the Luna 19 data N_e (black dots) and Luna 19 fit N_{Le} (solid line).

electrons emitted from the dust grains, as opposed to those collected from the ambient plasma (Goertz, 1989); and (ii) the inter-grain distances ($d > \sim 2$ cm) are much greater than the grain radii ($d \gg a$). Since the dust grain potential decreases as $\sim a/r$, where r is radial distance (Whipple, 1981; Goertz, 1989), the emitted dust-electrons effectively shield the charge on each dust grain within distances of just several grain radii. This means that from a charging perspective, the dust grains can be treated as being isolated from one another.

Using Eqs. (3) and (4), the column concentration of dust-electrons is

$$N_{de}(h) = \frac{4\pi\varepsilon_0}{e} a \langle \phi_d \rangle N_d(h); \tag{5}$$

where $\langle \phi_d \rangle$ is ϕ_d averaged along the line-of-sight, which implicitly acknowledges that there will be variations due to the individual charging history of each dust grain. For this initial analysis, we assume that $\langle \phi_d \rangle$ and a do not to vary with h, and that $N_d = N_{d\_A15}$.

The dashed line in Fig. 3b shows the N_{de} predictions calculated using Eq. (5) with $\langle \phi_d \rangle = 5$ V. The gray shading represents the estimated order-of-magnitude uncertainties associated with both the assumptions used in the dust-electron predictions and the unknown variations inherent when comparing the different dust populations present during the Apollo 15 and Luna 19 measurements, which were acquired almost a year apart. The black dots show the Luna 19 measurements, and the solid line is a fit to those measurements assuming an altitude profile for the electron concentration of,

$$n_{Le}(z) = n_{Le0} \exp\left[-\left(\frac{z}{H_{Le}}\right)^{\nu}\right]; \tag{6}$$

where ν is a dimensionless parameter, n_{Le0} is the concentration at the surface, and H_{Le} is a "scaling" height (distinct from H_d defined earlier). We find a good fit within the error bars using $\nu = 3$, $n_{Le0} = 950$ cm^{-3} and $H_{Le} = 25$ km, which we refer to as the Luna 19 fit.

From this initial comparison, it appears that the Luna 19 measurements are a factor of ≈ 20 greater than our Apollo 15 dust-electron predictions. Since we would not usually expect either a or $\langle \phi_d \rangle$ to vary significantly from our assumed values of 0.1 μm and 5 V, respectively, this suggests that the difference is more likely due to some combination of an under-estimation of the typical dust grain capacitance in Eq. (4), and exospheric dust being much more abundant during the measurements by Luna 19 than during those of Apollo 15 (see n_{d0} in Eq. (1) and Eq. (3)). Given the highly variable nature of the space environment at the Moon – and the significant uncertainties involved with this measurement comparison – an inferred factor ≈ 20 variation in exospheric dust concentrations alone seems plausible.

Above $h \approx 15$ km, the Luna 19 measurements decrease more rapidly with tangent height than the dust-electron predictions, which could be due to a decrease in a and/or $\langle \phi_d \rangle$ with altitude. A decrease in $\langle \phi_d \rangle$ could indicate that during the ejection process dust grains acquire a large positive potential from either tribo-electrification or some other mechanism, which is then reduced as they tend to a lower equilibrium potential in the solar wind. The precise details would depend on many factors, including dust charging timescales (Whipple, 1981). Another possible mechanism for ejecting positively charged dust could be associated with steep slopes near the lunar terminator that charge to positive potentials due to the increased incident solar UV flux and photoemission currents. However, the Luna 19 measurements do not appear to be consistent with dust charging from impact-generated plasmas (Horányi et al., 2009), which would tend to charge the dust negative unless the secondary emission yield is >1.

4. Electron concentrations in the lunar exosphere

In Fig. 4 we convert to volumetric concentrations in order to compare our predictions for dust-electrons and the Luna 19 fit with the typical solar wind background of 5 cm^{-3}, and two of the other suggested mechanisms: photo-ionization of exospheric neutrals and photoemission from the surface. Since argon is the most abundant exospheric specie at sunrise (Stern, 1999), we have assumed that it dominates the production of electrons from the photo-ionization of exospheric neutrals (see Vondrak, 1992). At $SZA \approx 89^{\circ}$, the surface will likely have been charged $\sim$10–100 V negative (Halekas et al., 2008). The concentration of photoelectrons was calculated assuming a surface potential of 30 V negative and $\lambda_D = 10$ m (Nitter et al., 1998). These two estimates likely represent typical upper limits.

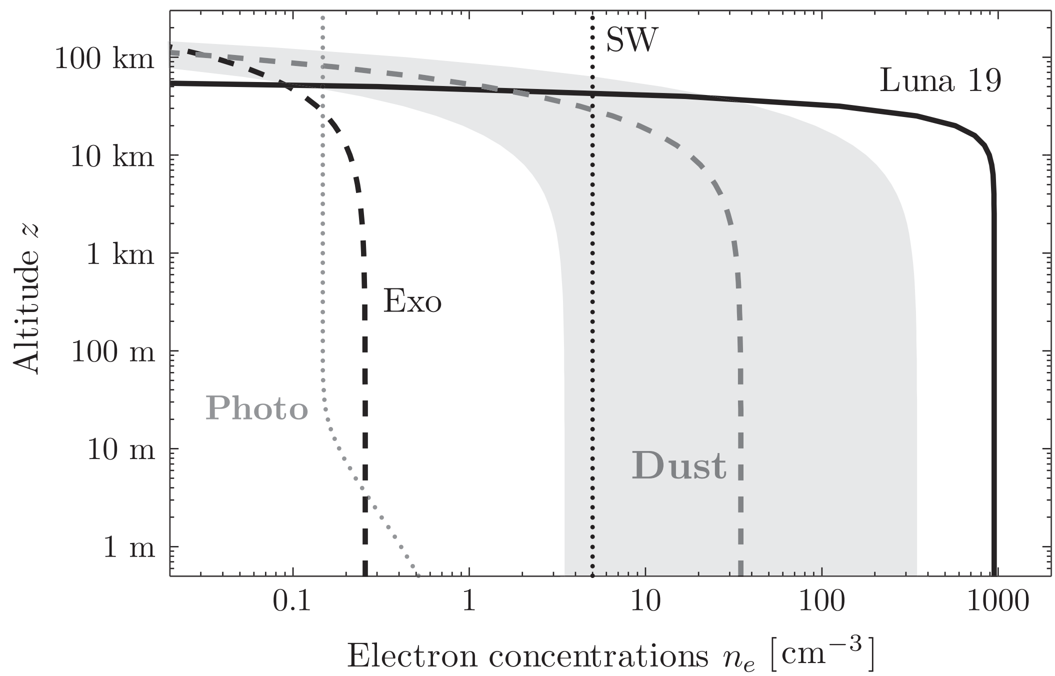

Fig. 4. Predicted electron concentrations in the lunar exosphere due to: photoemission from the lunar surface (gray dotted line); photo-ionization of exospheric neutrals (black dashed line); typical background solar wind (black dotted line); dust-electrons based on Apollo 15 dust measurements (dashed lines) with estimates uncertainties (gray shading), and the fit to the Luna 19 measurements (black solid line). These results suggest that dust-electrons are the most likely cause of the Luna 19 measurements.

The order-of-magnitude comparison presented in Fig. 4 strongly suggests that dust-electrons are a more plausible source for the electrons measured by Luna 19 than either the photo-ionization of exospheric neutrals or photoelectrons from the surface. In fact, the electrons produced by these other processes would be undetectable by the radio occultation technique. Secondary electrons emitted from the surface would have the same altitude profile as the photoelectrons and comparable concentrations, so this is also unlikely to be a significant source.

5. Discussion

In this section we briefly discuss some of the other relevant observations and mechanisms, as well as possible consequences for a lunar ionosphere dominated by dust-electrons.

Some of the electron concentration profiles inferred from Luna 19 and 22 observations indicated that the peak concentration could occur well above the surface; e.g., the Luna 22 observations on 17 August 1974 indicated a peak at ~25 km altitude (Vyshlov, 1976). In this case, the tangent point ($SZA \approx 94^{\circ}$) was ~4 km below the lunar sunlight/shadow boundary, so the radio signals would have partially traversed the Moon's shadow where there is no solar UV to produce photo-emitted dust-electrons. This would have the greatest effect at the smallest tangent heights, which would explain the apparent decrease in electrons close to the surface. Therefore, these observations are consistent with the dust-electron model.

An important mechanism that we have not considered here is the trapping of electrons produced by the photo-ionization of exospheric neutrals in crustal magnetic fields with strengths at the surface of ~100 nT and scale sizes of ~100 km. Savich (1976) suggested that this could explain concentrations of $\sim 10^3$ cm^{-3} at altitudes of up to 10 km; however, given the assumed magnetic field configuration, production rate of exospheric ions and uncertainties in trapping efficiencies, this suggestion could be an over-estimate by a factor of ~100–1000. Even though a crustal field associated with Abel crater at ~30°S, 90°E (Richmond and Hood, 2008) has been detected about ~350 km from the Luna 19 tangent point, it probably had a negligible influence on the measurements.

Electron populations similar to the Luna 19 measurements have so far evaded direct detection, despite Lunar Prospector (LP) having reached altitudes of ≈ 17 km. This is likely because the LP Electron Reflectometer (ER) energy threshold was ~7 eV at best, which is well above the electron energies expected for either photoemission (~2 eV) or secondary emission (~5 eV) from lunar dust, and so any ambient dust-electrons would have been undetectable. In addition, the lower ER energy channels would have been swamped by photoelectrons from LP when in sunlight (Halekas et al., 2008).

Preliminary results indicate that the electron concentrations inferred from the radio occultation measurements by Kaguya were lower than those inferred from the Luna missions, with temporal variations in the Earth's ionosphere representing the most significant source of uncertainty (Imamura et al., 2010). From Table 1, we note that the $F_{10.7}$ index (solar UV proxy) was particularly low during the Kaguya mission, since it coincided with an exceptionally quiet solar minimum. This indicates that photoemission would have been weaker – and the associated photoelectron concentrations reduced – compared with the Luna and Apollo observations. In addition, this could have resulted in a decrease in dust lofting activity (Stubbs et al., 2006), thus contributing to a further reduction in dust and dust-electron concentrations. The preliminary Kaguya results possibly suggest a tendency toward higher concentrations at lunar sunrise (Imamura et al., 2008). Such a tendency would also be consistent with a dust-electron source, since analyses of both the Apollo 17 LEAM measurements and Apollo coronal photographs have indicated greater exospheric dust activity around sunrise than sunset (Berg et al., 1976; Glenar et al., 2011).

There could be other consequences related to the presence of charged dust and dust-electrons in the lunar exosphere, such as mass loading of the ambient plasma flow that would locally reduce the flow velocity and compress the magnetic field. Exospheric dust could also act as a source of sputtered neutrals and ions, which would represent another source of electrons.

6. Conclusions

Dust-electrons produced by photoemission and secondary emission from exospheric dust could well be responsible for the high concentrations of electrons inferred from the radio occultation experiments on Luna 19 and 22. The dust-electron predictions discussed here significantly exceed reasonable estimates for any of the other suggested mechanisms. They also suggest that exospheric dust concentrations during the Luna 19 electron measurements could have been up to a factor of ≈ 20 higher than during the Apollo 15 dust measurements.

The dust-electron model is able to maintain much higher electron concentrations compared with other mechanisms because the electric field local to a positively charged dust grain ($\sim \phi_d/a$) dominates over the plasma convection electric field, which means that most dust-electrons are recycled and very few are lost to the ambient plasma. This model is also consistent with the inferred Luna electron populations only being present in sunlight (Vasil'ev et al., 1974), since in shadow dust grains become electron collectors as opposed to electron emitters (Goertz, 1989; Farrell et al., 2009). These results suggest a new paradigm in which exospheric dust can dominate the formation and evolution of a highly variable lunar ionosphere.

Charged dust and dust-electron signatures could be present in other lunar datasets, and may be detectable by future missions such as ARTEMIS and LADEE. However, to fully understand the lunar ionosphere will require further orbital and landed experiments, such as simultaneous radio occultation and multi-wavelength optical measurements to constrain the size, concentration and charge state of the exospheric dust population.

Acknowledgments

Research was funded by NASA Grants: NNX08AM76G, NNX07AG10G, NNX08BA32G, and NNX09AG78A. We benefitted from access to NASA/OMNIWeb, as well as from useful discussions with J.K. Burchill and helpful suggestions from the reviewers.

References

Bauer, S.J., 1996. Limits to a lunar ionosphere. Anz. Abt. II 133, 17–21.
Berg, O.E., et al., 1976. Lunar soil movement registered by the Apollo 17 cosmic dust experiment. In: Elsasser, H., Fechtig, H. (Eds.), Interplanetary Dust and Zodiacal Light. Springer-Verlag, pp. 233–237, A76-4370122-90.
Chamberlain, J.W., 1978. Theory of Planetary Atmospheres: An Introduction to their Physics and Chemistry. Academic Press, ISBN: 0-12-167250-6.
Collier, M.R., Stubbs, T.J., 2009. Neutral solar wind generated by lunar exospheric dust at the terminator. J. Geophys. Res. 114, A01104. doi:10.1029/2008JA013716.
Elsmore, B., 1957. Radio observations of the lunar atmosphere. Phil. Mag. 2, 1040–1046.
Farrell, W.M., et al., 2009. Electron density dropout near Enceladus in the context of watervapor and waterice. Geophys. Res. Lett. 36, L10203. doi:10.1029/2008GL037108.
Glenar, D.A., et al., 2011. A reanalysis of the Apollo light scattering observations, and implications for lunar exospheric dust. Planet. Space Sci.. doi:10.1016/j.pss.2010.12.003.
Goertz, C.K., 1989. Dusty plasmas in the solar system. Rev. Geophys. 27 (2), 271–292.
Halekas, J.S., et al., 2008. Lunar Prospector observations of the electrostatic potential of the lunar surface and its response to incident currents. J. Geophys. Res. 113, A09102. doi:10.1029/2008JA013194.
Horányi, M., et al., 2009. Impact generated plasmas on the lunar surface. Eos Trans. AGU 90 (52) (Fall Meet. Suppl., P32A-04).
Imamura, T., et al., 2008. Studying the lunar ionosphere with SELENE radio science experiment. Eos Trans. AGU 89 (53) (Fall Meet. Suppl., P51D-04).
Imamura, T., et al., 2010. Studying the lunar ionosphere with SELENE radio science experiment. Space Sci. Rev.. doi:10.1007/s11214-010-9660-0.
McCoy, J.E., 1976. Photometric studies of light scattering above the lunar terminator from Apollo solar corona photography. In: Proceedings of the Seventh Lunar Science Conference, pp. 1087–1112.
Nitter, T., et al., 1998. Levitation and dynamics of charged dust in the photoelectron sheath above surfaces in space. J. Geophys. Res. 103, 6605–6620.
Park, J.S., et al., 2006. Micro-morphology and toxicological effects of lunar dust. In: Proceedings of the 37th Lunar and Planetary Science Conference, Abstract no. 2193.
Richmond, N.C., Hood, L.L., 2008. A preliminary global map of the vector lunar crustal magnetic field based on Lunar Prospector magnetometer data. J. Geophys. Res. 113, E02010. doi:10.1029/2007JE002933.
Savich, N.A., 1976. Cislunar plasma model. Space Res. XVI, 941–943.
Stern, S.A., 1999. The lunar atmosphere: history, status, current problems, and context. Rev. Geophys. 37 (4), 453–491.
Stubbs, T.J., et al., 2006. A dynamic fountain model for lunar dust. Adv. Space Res. 37 (1), 59–66.
Vasil'ev, M.B., et al., 1974. Radio transparency of circumlunar space using the Luna-19 station. Cosmic Research 12, 102–107.
Vondrak, R.R., 1992. Lunar base activities and the lunar environment. In: Proceedings of the Second Conference on Lunar Bases and Space Activities of the 21st Century, vol. 1, pp. 337–345.
Vyshlov, A.S., 1976. Preliminary results of circumlunar plasma research by the Luna 22 spacecraft. Space Res. XVI, 945–949.
Vyshlov, A.S., Savich, N.A., 1979. Observations of radio source occultations by the Moon and the nature of the plasma near the Moon. Cosmic Res. 16, 450–454.
Whipple, E.C., 1981. Potentials of surfaces in space. Rep. Prog. Phys. 44, 1197–1250.